Frustrated Magnetism and Quantum Spin Liquid Phase

Daniel Wong
(Dated: December 19, 2020)

Frustrated systems are characterized by a large degeneracy of their ground state, which manifests as an extensive residual entropy at zero temperature. Such degeneracy arises due to the inability to simultaneously minimize the energy due to competing interactions present within the system. In the context of frustrated magnetic systems, magnetic moments tend to remain disordered and the system fails to obtain long-range order down to low temperatures. For the purpose of this report, we will limit the discussion of frustrated magnetism to a certain class of materials known as "rare-earth pyrochlores", which exhibits many interesting behaviours that have been subject to study for the past few decades. Other classes of frustrated magnets, such as Kitaev magnets, also exist, but will not be explored for this discussion. We will also briefly discuss the quantum spin liquid phase and how certain rare-earth pyrochlores serve as potential candidates for being quantum spin liquids.

I. INTRODUCTION

Before embarking on a discussion of frustrated magnetic systems, it may be illustrative to show an example of frustration through a simple model. Consider three Ising spins lying on the vertices of an equilateral triangle. If one considers only the nearest-neighbour Ising interaction between all three spins, the system can be described by the Hamiltonian

$$\mathcal{H} = -J \sum_{\langle ij \rangle} \sigma_i^z \sigma_j^z$$

where $\sigma_i^z = \pm 1$ describes the Ising spin and J can be ferromagnetic ($J > 0$) or anti-ferromagnetic ($J < 0$).

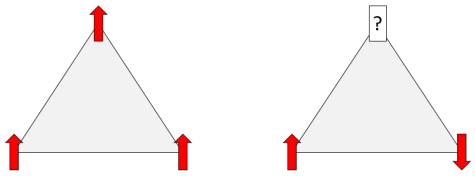

(a) (b)

FIG. 1: Ising spins with (a) ferromagnetic interactions and (b) anti-ferromagnetic interactions

When $J > 0$, the interaction between two spins is minimized when both spins are aligned and the total energy becomes minimized when all spins align. When $J < 0$, the interaction between two spins is minimized when both spins are anti-aligned. On a triangular plaquette (see Fig. 1), two spins may anti-align to minimize their interaction but the third spin will fail to simultaneously anti-align with the other two spins, leading to a *frustrated system*. If one extends the system of Ising spins on a triangular plaquette into a system of spins on a triangular lattice, the degeneracy of the ground state exponentially increases with the number of Ising spins N. In this way, frustration leads to an extensive residual entropy. This idea may then be generalized to more complicated systems.

II. THEORY

Lattice

For this report, we will focus on a class of frustrated magnets known as "rare-earth pyrochlores". Rare-earth pyrochlores follow the general chemical formula $R_2M_2O_7$, where R describes a trivalent rare-earth metal and M describes a tetravalent transition metal, with either element serving as the magnetic ion[1]. Both R and M separately form corner-sharing networks of tetrahedra (known as the pyrochlore lattice) that interpenetrate with each other. The remaining oxygen atoms serve as a crystal field that surrounds each ion[1].

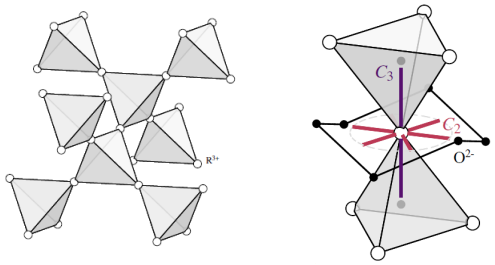

(a) (b)

FIG. 2: (a) Corner-sharing tetrahedra network[2] (b) Surrounding oxygen atoms for the R^{3+} ion[2]

Hamiltonian

Consider the magnetic ions on the pyrochlore lattice. For rare-earth pyrochlores, their energy is largely determined by Coulomb interaction and spin-orbit coupling. Taking the total angular momentum, $\mathbf{J} = \mathbf{L} + \mathbf{S}$ to be a good quantum number, following Hund's rule gives a $2J + 1$-degenerate ground-state manifold for each ion[1]. This degeneracy is lifted by the crystal field potential due to the surrounding ions[3], which is given by the Hamiltonian

$$\begin{aligned}\mathcal{H}_{\text{cf}} = {} & B_{20}O_{20}(\mathbf{J}) + B_{40}O_{40}(\mathbf{J}) + B_{43}O_{43}(\mathbf{J}) \\ & + B_{60}O_{60}(\mathbf{J}) + B_{63}O_{63}(\mathbf{J}) + B_{66}O_{66}(\mathbf{J})\end{aligned}$$

where B_{KQ} are constants found experimentally and $O_{KQ}(\mathbf{J})$ are Stevens operator equivalents of the total angular momentum operator $\mathbf{J}$ (see Appendix A)[4]. Note that $\mathbf{J}$ is defined with respect to the local axes of each ion and not to the global axes of the system (see Appendix B). For most rare-earth pyrochlores, the lifting of the $2J+1$-degeneracy leads to a ground state doublet, which will be denoted as $|+\rangle$ and $|-\rangle$[2].

The next important interaction arises as a pair-wise interaction between the ions. In general, this interaction arises as a multipolar exchange given by[5]

$$\mathcal{H}_{\text{ex}} = \sum_{ij} \sum_{KQ} \sum_{K'Q'} \mathcal{M}_{ij}^{KQ;K'Q'} \mathcal{O}_{KQ}(\mathbf{J}_i) \mathcal{O}_{K'Q'}(\mathbf{J}_j)$$

where $\mathcal{M}_{ij}^{KQ;K'Q'}$ are constants and $\mathcal{O}_{KQ}(\mathbf{J})$ are multipole operators of the total angular momentum operator $\mathbf{J}$. Note that $\mathbf{J}$ is now defined with respect to some global axes. Given the difference in energy scale between $\mathcal{H}_{\text{ex}}$ and $\mathcal{H}_{\text{cf}}$, one can find an effective Hamiltonian using Brillouin-Wigner perturbation theory

$$\mathcal{H}_{\text{eff}} = \mathcal{H}_0 + P_0 V P_0 + P_0 V \frac{1-P_0}{E_0 - \mathcal{H}_0} V P_0 + \dots$$

where the unperturbed Hamiltonian $\mathcal{H}_0$ is taken to be the crystal-field Hamiltonian $\mathcal{H}_{cf}$ and the perturbation V is the exchange Hamiltonian $\mathcal{H}_{ex}$. P_0 is the projector into the ground-state manifold spanned by the local ground-state doublet $|\pm\rangle$ of each magnetic ion.

For most rare-earth pyrochlores (with the exception of $Tb_2Ti_2O_7$ and related material[6]), the lowest-lying doublet is well-separated from higher energy levels. Thus, the effective model can be taken only to first-order in perturbation theory. If one only includes nearest-neighbour interactions, the effective Hamiltonian becomes

$$\begin{aligned}\mathcal{H}_{\text{eff}} = \sum_{\langle ij \rangle} \big[& J_{zz} S_i^z S_j^z - J_{\pm}(S_i^+ S_j^- + \text{h.c.}) \\ & + J_{\pm\pm}(\gamma_{ij} S_i^+ S_j^+ + \text{h.c.}) \\ & + J_{z\pm}(\zeta_{ij}[S_i^z S_j^+ + S_i^+ S_j^z] + \text{h.c.})\big]\end{aligned}$$

where S_i are pseudo-spin operators defined by

$$S^z \equiv \frac{|+\rangle\langle+| - |-\rangle\langle-|}{2} \qquad S^{\pm} \equiv |\pm\rangle\langle\mp|$$

and γ_{ij} and ζ_{ij} are bond-dependent constants. From this effective model, the models used for different rare-earth pyrochlores can be obtained by appropriately setting the coupling constants J_{zz}, $J_{\pm}$, $J_{\pm\pm}$, and $J_{z\pm}$ to experimental data. In general, these interactions amongst nearest-neighbour pairs will compete and lead to a frustrated system. Note that these terms are generated due to first-order perturbation theory. In the event that the ground-state doublet is not well-separated from the excited states (as is the case in material such as $Tb_2Ti_2O_7$), perturbation theory must be taken to higher order and further terms may be generated.

III. CLASSICAL SPIN ICE

Let us consider the effective model for $Ho_2Ti_2O_7$, which historically was the first example of a rare-earth pyrochlore to be found[7]. Along with $Dy_2Ti_2O_7$, $Ho_2Ti_2O_7$ is considered to be a typical example of a *classical spin ice*. The local crystal field environment causes the magnetic Ho^{3+} (or Dy^{3+} in the case of $Dy_2Ti_2O_7$) ions to strongly align along its local z-axis and allows the effective Hamiltonian to be approximated by only the J_{zz} term[7]. This alignment causes the magnetic moment of each ion to point either into or out of the tetrahedra that they lie on.

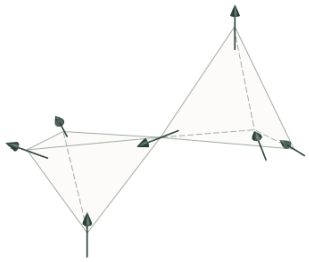

FIG. 3: Magnetic moments pointing into or out of corner-sharing tetrahedra[8]

Classical spin ice can be mapped directly onto an antiferromagnetic Ising model on a pyrochlore lattice, similar to one proposed by Anderson in 1956[9]. This model obtains a residual entropy similar to that of water ice predicted by Pauling[10]. Additionally, the ground states of classical spin ice are found when the magnetic moments are arranged such that every tetrahedron contains two moments pointing "in" and two moments pointing "out" of every tetrahedron[7]. This condition maps onto the Bernal-Fowler ice rules that are used to describe proton disorder in the ground state of water ice[11]. These similarities to water ice serve as the etymological basis behind the name *spin ice*.

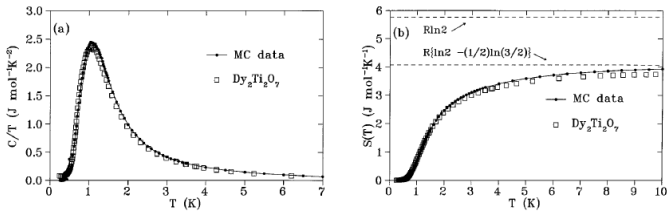

FIG. 4: Quantitative agreement of (a) specific heat and (b) entropy between experimental data and Monte Carlo simulations of dipolar spin ice for $Dy_2Ti_2O_7$[12]

Magnetic Monopole-Like Excitations

Consider an excitation of the system out of its ground state manifold. Such an excitation arises as a flip in magnetic moments, such that two adjacent tetrahedra no longer satisfy the "two-in, two-out" constraint required to obtain the ground state.

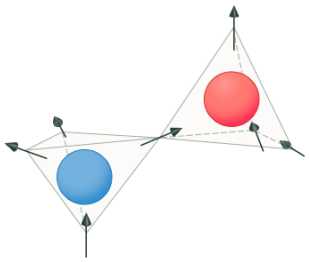

FIG. 5: Excitation with a source (blue) and sink (red) of magnetization $\mathbf{M}$[8]

These tetrahedra can be viewed as being a "source" or "sink" of magnetization $\mathbf{M}$, which allows a "magnetic charge" $\pm Q$ to be assigned to either tetrahedra[13]. These charges may diffuse apart by successively flipping magnetic moments such that the tetrahedra violating the two-in, two-out constraint become spatially separated[14].

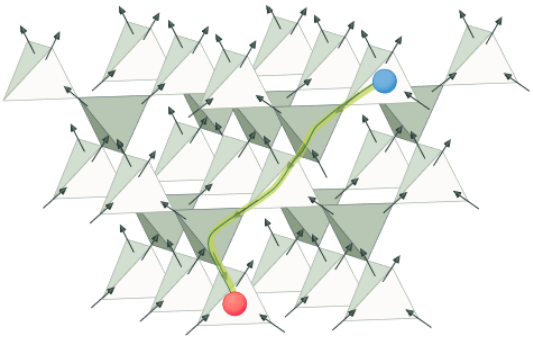

FIG. 6: Separation of magnetic charges[8]

One can calculate an effective interaction $-\mu_0 Q^2/(4\pi r)$ that resembles a magnetic Coulomb interaction between the pair of charges separated by a distance r[15]. Given this similarity to the magnetic monopoles introduced by Dirac in his modification of Maxwell's equations[16], these magnetic charges have been termed *monopoles*. Note that these monopoles are not true magnetic monopoles given that these charges act as sources and sinks for $\mathbf{M}$. The Maxwell equation $\nabla \cdot \mathbf{B} = 0$ is still satisfied within the material.

IV. QUANTUM SPIN ICE

In general, rare-earth pyrochlores need not be strictly Ising-like and may include non-negligible contributions from all four terms in the effective Hamiltonian. The ground state of the effective model can achieve a variety of phases as one explores the parameter space.

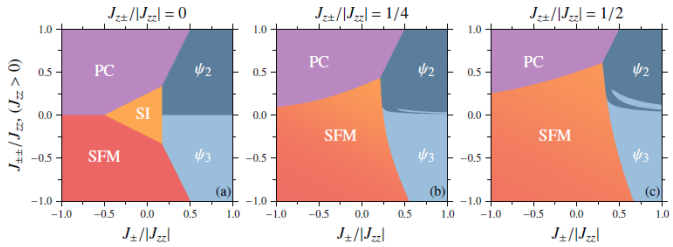

FIG. 7: Phase diagram for the effective model with $J_{zz} > 0$ given different coupling constant values. Note the spin ice (SI) phase, which entails the ground state of classical spin ice described in the previous section[2]. Other phases listed include the Palmer-Chalker (PC) phase and the splayed ferromagnet (SFM) phase.

In the interest of brevity for this report, we will avoid discussing many of the possible examples of rare-earth pyrochlores that can fall into the different phase classifications. Instead, we will concentrate on a select number of rare-earth pyrochlores which serve as candidates for obtaining a *quantum spin liquid phase*.

Quantum Spin Liquid Phase

A proper derivation of the quantum spin liquid phase will lie beyond the scope of this report. As such, only the general ideas and properties of the quantum spin liquid phase will be described here.

In 1973, Anderson proposed an alternative ground state to the anti-ferromagnetic Néel state for the anti-ferromagnetic Heisenberg model on the triangular lattice for spin-$\frac{1}{2}$ particles. This alternative ground state was the resonating valence bond (RVB) state and is the first example of a quantum spin liquid. Such a state is composed of superpositions of singlet states that span the entire lattice[17]. The idea of quantum spin liquids later gathered much scientific interest when Anderson hypothesized that the high-temperature superconducting properties of $La_2Cu_2O_4$ may be attributable to it being in an RVB state[18]. In the context of rare-earth pyrochlores, much scientific research is going into experimentally realizing such a phase in a pyrochlore material.

The quantum spin liquid phase is described by a collective paramagnetic state that avoids all spontaneous symmetry-breaking down to zero temperature, in contrast to other ordered states that can be characterized with a local order parameter[19]. Note the quantum spin

liquid phase differs from the typical spin liquid phase obtained in classical spin ice. In classical spin ice, classical fluctuations freeze out once the energy k_BT becomes sufficiently small. In a quantum spin liquid phase, spins are still free to fluctuate due to the zero-point motion associated with quantum fluctuations[20]. In terms of properties, quantum spin liquids obtain fractionalized excitations that have photon-like dispersion and the spin degrees of freedom encounter significant correlations and long-range quantum entanglement[21].

Candidates

Identifying a quantum spin liquid phase becomes difficult experimentally due to the lack of a tell-tale marker typical to ordered states. This is tantamount to confirming no magnetic ordering occurs down to zero temperature[22] . Operationally, one can confirm this through thermodynamic measurements and probing with nuclear magnetic resonance or muon-spin resonance[20]. This lack of magnetic ordering has led to many rare-earth pyrochlores being proposed as a candidate for the quantum spin liquid phase.

$Tb_2\,Ti_2\,O_7$

$Tb_2Ti_2O_7$ is found to remain paramagnetic down to 70 mK[23] and obtains significant spin correlations down to low temperatures[24], which is signature of a quantum spin liquid phase. Thus, $Tb_2Ti_2O_7$ was one of the first proposed candidates of a rare-earth pyrochlore to host a quantum spin liquid phase. However, attempts to understand its ground state using the effective Hamiltonian have been unsuccessful. One issue arises due to the low-lying first excited doublet after the $2J+1$-degenerate ground-state manifold has been lifted by the crystal field[6]. As previously mentioned, the effective Hamiltonian was taken only to first order in perturbation theory due to the clear separation in energy between the ground state and higher excited states. In the case where the ground state and higher excited states are of comparable magnitude in energy, higher order terms in the perturbation theory can no longer be ignored. These higher order terms generate effective three-body pseudospin terms that can affect the description of the ground state in $Tb_2Ti_2O_7$[25].

$Pr_2\,Zr_2\,O_7$

$Pr_2Zr_2O_7$ is another candidate for a quantum spin liquid, with no indication of long-range ordering down to 20 mK[26]. Likewise, thermal conductivity is found to suddenly increase going below 200 mK, which is interpreted to be sign of a quantum spin liquid ground state[27]. However, inelastic neutron scattering reveals a broad magnetic Bragg peak at [200], indicating a slight structural disorder to the pyrochlore lattice in the material[28]. This structural disorder acts as a random transverse field on the magnetic ions and requires a modification of the effective Hamiltonian that is used to describe other rare-earth pyrochlores[28].

V. CONCLUSION

Rare-earth pyrochlores are a class of frustrated magnets that have been studied for the past couple of decades. Most rare-earth pyrochlores are successfully described by an effective model that can be tuned to match experimental data. This model itself has a rich phase diagram that can exhibit many interesting properties, such as order by disorder in $Er_2Ti_2O_7$[29] or multiphase competition in $Yb_2Ti_2O_7$[30]. One such phase is the quantum spin liquid phase, with active areas of research trying to experimentally realize this phase in rare-earth pyrochlores.

Appendix A: Stevens Operator Equivalents

The Stevens operator equivalents $O_{lm}(\mathbf{J})$ in the crystal field Hamiltonian $\mathcal{H}_{cf}$ are given by[31]

$$
\begin{aligned}
O_{20}(\mathbf{J}) &= 3\mathbf{J}_z^2 - X \\
O_{40}(\mathbf{J}) &= 35\mathbf{J}_z^4 - (30X-25)\mathbf{J}_z^2 + 3X^2 - 6X \\
O_{43}(\mathbf{J}) &= \frac{1}{4}[(\mathbf{J}_+^3 + \mathbf{J}_-^3)\mathbf{J}_z + \mathbf{J}_z(\mathbf{J}_+^3 + \mathbf{J}_-^3)] \\
O_{60}(\mathbf{J}) &= 231\mathbf{J}_z^6 - (315X-735)\mathbf{J}_z^4 + (105X^2 - 525X + 294)\mathbf{J}_z^2 \\
&\quad - 5X^3 + 40X^2 - 60X \\
O_{63}(\mathbf{J}) &= \frac{1}{4}[(\mathbf{J}_+^3 + \mathbf{J}_-^3)(11\mathbf{J}_z^3 - (3X+59)\mathbf{J}_z) \\
&\quad + (11\mathbf{J}_z^3 - (3X+59)\mathbf{J}_z)(\mathbf{J}_+^3 + \mathbf{J}_-^3)] \\
O_{66}(\mathbf{J}) &= \frac{1}{2}(\mathbf{J}_+^6 + \mathbf{J}_-^6)
\end{aligned}
$$

where $\mathbf{J}_\pm = \mathbf{J}_x \pm i\mathbf{J}_y$ and $X = J(J+1)$ are the eigenvalues of $\mathbf{J}^2$. In general, the Stevens operators are related to the tesseral harmonics through the replacement of its position variables by the symmetrized operator equivalent in total angular momentum operators. More technical details in obtaining the operator equivalents are contained in the original paper by Stevens[4].

In the case of rare-earth pyrochlores, the atoms crystallize in a $Fd\bar{3}m$ space group. In order to respect the D_{3d} point symmetry of the magnetic ion, the crystal field Hamiltonian must be composed of Stevens operator equivalents that respect the same symmetry. The Stevens operator equivalents listed above are the only ones allowed by symmetry[1].

Appendix B: Local Axes

Consider the orientation of oxygen atoms around the magnetic ions (see Fig. 2b). Relative to the line connecting the magnetic ion to the centre of the tetrahedron, the surrounding oxygen atoms will be oriented in the same manner for all magnetic ions. However, this line does not uniformly point along some global axis for each ion. Therefore, a crystal field Hamiltonian written in terms of *global* total angular momentum operators $\tilde{\mathbf{J}}$ will vary depending on the ion being described.

One can instead define a crystal field Hamiltonian in terms of *local* total angular momentum operators $\mathbf{J}$, where the momentum operators are defined relative to the line connecting the centre of the tetrahedron to each corresponding magnetic ion. Such a Hamiltonian will now be the same for all magnetic ions on the pyrochlore lattice. Thus, it becomes convenient to define a set of local axes for each ion.

Given that there are only four possible directions for this line (corresponding with the centre of the tetrahedron point to any one of the four corners of the tetrahedron), only four set of local axes need to be defined. Many possible conventions exist in the literature[32], though for the purpose of this report, we will use the conventions defined by Ross et al[33]. For atoms located at the four corners given by position vectors

$$\begin{aligned}\mathbf{r}_1 &= \frac{a}{8}(1,1,1)\\ \mathbf{r}_2 &= \frac{a}{8}(1,-1,-1)\\ \mathbf{r}_3 &= \frac{a}{8}(-1,1,-1)\\ \mathbf{r}_4 &= \frac{a}{8}(-1,-1,1)\end{aligned}$$

where a is some lattice constant, the corresponding local axes are

$$\begin{aligned}\hat{z}_1 &= \frac{1}{\sqrt{3}}(1,1,1), & \hat{x}_1 &= \frac{1}{\sqrt{6}}(-2,1,1)\\ \hat{z}_2 &= \frac{1}{\sqrt{3}}(1,-1,-1), & \hat{x}_1 &= \frac{1}{\sqrt{6}}(-2,-1,-1)\\ \hat{z}_3 &= \frac{1}{\sqrt{3}}(-1,1,-1), & \hat{x}_1 &= \frac{1}{\sqrt{6}}(2,1,-1)\\ \hat{z}_4 &= \frac{1}{\sqrt{3}}(-1,-1,1), & \hat{x}_1 &= \frac{1}{\sqrt{6}}(2,-1,1)\end{aligned}$$

with $\hat{y}_i = \hat{z}_i \times \hat{x}_i$. Note that the ground state doublet $|\pm\rangle$ will be written in the basis of the projection of $\mathbf{J}$ on the local $\hat{z}$-axis of each ion, rather than some global $\hat{z}$-axis.

Appendix C: Example Calculation

In order to highlight some of the more technical details in obtaining an effective Hamiltonian, an example calculation will be performed in this section. Let us consider an interaction, where after being rewritten in terms of the local bases given in Appendix B, yields a Heisenberg-like exchange between two atoms, labeled with site index 1 and 2.

$$\begin{aligned}\mathcal{H}_{\text{ex}} &= \mathbf{J}_1 \cdot \mathbf{J}_2\\ &= \frac{1}{2}(\mathbf{J}_{+,1}\mathbf{J}_{-,2} + \mathbf{J}_{-,1}\mathbf{J}_{+,2}) + \mathbf{J}_{z,1}\mathbf{J}_{z,2}\end{aligned}$$

The ground-state manifold of both atoms is spanned by the states

$$\begin{aligned}|\psi_{0,1}\rangle &= |+\rangle_1 \otimes |+\rangle_2\\ |\psi_{0,2}\rangle &= |+\rangle_1 \otimes |-\rangle_2\\ |\psi_{0,3}\rangle &= |-\rangle_1 \otimes |+\rangle_2\\ |\psi_{0,4}\rangle &= |-\rangle_1 \otimes |-\rangle_2\end{aligned}$$

Thus, the projector into the ground-state manifold of both atoms is given by

$$P_0 = |\psi_{0,1}\rangle\langle\psi_{0,1}| + |\psi_{0,2}\rangle\langle\psi_{0,2}| + |\psi_{0,3}\rangle\langle\psi_{0,3}| + |\psi_{0,4}\rangle\langle\psi_{0,4}|$$

The first-order term $P_0\mathcal{H}_{\text{ex}}P_0$ in the perturbation theory will lead to the generation of many different terms. Let us consider the calculation of one such term.

$$
\begin{aligned}
P_0\mathcal{H}_{\rm ex}P_0 &= \ldots + |\psi_{0,2}\rangle\langle\psi_{0,2}|\,\frac{1}{2}\mathbf{J}_{+,1}\mathbf{J}_{-,2}\,|\psi_{0,3}\rangle\langle\psi_{0,3}| + \ldots \\
&= \ldots + \left(\frac{1}{2}\,|+\rangle_{1\,1}\,\langle+|\,\mathbf{J}_{+,1}\,|-\rangle_{1\,1}\,\langle-|\right)\otimes\left(\frac{1}{2}\,|-\rangle_{2\,2}\,\langle-|\,\mathbf{J}_{-,2}\,|+\rangle_{2\,2}\,\langle+|\right) + \ldots \\
&= \ldots + \left(\frac{1}{4}{}_1\,\langle+|\mathbf{J}_{+,1}|-\rangle_{1\;2}\,\langle-|\mathbf{J}_{-,2}|+\rangle_2\right)\underbrace{|+\rangle_{1\;\,1}\langle-|}_{S_1^+}\otimes\underbrace{|-\rangle_{2\;\,2}\langle+|}_{S_2^-} + \ldots \\
&= \ldots + \left(\frac{1}{4}{}_1\,\langle+|\mathbf{J}_{+,1}|-\rangle_{1\;2}\,\langle-|\mathbf{J}_{-,2}|+\rangle_2\right)S_1^+S_2^- + \ldots
\end{aligned}
$$

The matrix elements present before the pseudospin terms will generate a numerical prefactor that depends on the details of the ground-state doublet $|\pm\rangle$ and the local total angular momentum operator $\mathbf{J}$. After performing a similar calculation for all of the generated terms due to the first-order term and collecting similar pseudospin terms, one will find that the first-order term will obtain the form given earlier for the effective Hamiltonian

$$P_0\mathcal{H}_{\rm ex}P_0 = J_{zz}S_1^zS_2^z - J_{\pm}(S_1^+S_2^- + \text{h.c.}) + J_{\pm\pm}(\gamma_{12}S_1^+S_2^+ + \text{h.c.}) + J_{z\pm}(\zeta_{12}[S_1^zS_2^+ + S_1^+S_2^z] + \text{h.c.})$$

Note that the calculation above was performed for a single interaction between one pair of atoms. In the context of rare-earth pyrochlores, the above procedure must be performed for all possible nearest-neighbour interactions.

[1] J. S. Gardner, M. J. P. Gingras, and J. E. Greedan, Reviews of Modern Physics **82**, 53 (2010).
[2] J. G. Rau and M. J. Gingras, Annual Review of Condensed Matter Physics **10**, 357 (2019).
[3] D. J. Newman and B. Ng, *Crystal Field Handbook* (Cambridge University Press, 2000).
[4] K. W. H. Stevens, Proceedings of the Physical Society. Section A **65**, 209 (1952).
[5] N. Iwahara and L. F. Chibotaru, Physical Review B **91**, 174438 (2015).
[6] J. Zhang, K. Fritsch, Z. Hao, B. V. Bagheri, M. J. P. Gingras, G. E. Granroth, P. Jiramongkolchai, R. J. Cava, and B. D. Gaulin, Physical Review B **89**, 134410 (2014).
[7] M. J. Harris, S. T. Bramwell, D. F. McMorrow, T. Zeiske, and K. W. Godfrey, Physical Review Letters **79**, 2554 (1997).
[8] M. J. P. Gingras, Science **326**, 375 (2009).
[9] P. W. Anderson, Physical Review **102**, 1008 (1956).
[10] L. Pauling, Journal of the American Chemical Society **57**, 2680 (1935).
[11] J. D. Bernal and R. H. Fowler, The Journal of Chemical Physics **1**, 515 (1933).
[12] B. C. den Hertog and M. J. P. Gingras, Physical Review Letters **84**, 3430 (2000).
[13] M. J. P. Gingras, Physics in Canada **68** (2012).
[14] T. Fennell, P. P. Deen, A. R. Wildes, K. Schmalzl, D. Prabhakaran, A. T. Boothroyd, R. J. Aldus, D. F. McMorrow, and S. T. Bramwell, Science **326**, 415 (2009).
[15] C. Castelnovo, R. Moessner, and S. L. Sondhi, Nature **451**, 42 (2008).
[16] P. A. M. Dirac, Proceedings of the Royal Society A **133**, 60 (1931).
[17] P. W. Anderson, Materials Research Bulletin **8**, 153 (1973).
[18] P. W. Anderson, Science **235**, 1196 (1987).
[19] G. Misgulch, "Quantum spin liquids and fractionalization," in *Introduction to Frustrated Magnetism: Materials, Experiments, Theory*, edited by C. Lacroix, P. Mendels, and F. Mila (Springer Berlin Heidelberg, Berlin, Heidelberg, 2011) pp. 407–435.
[20] L. Balents, Nature **464**, 199 (2010).
[21] M. J. P. Gingras and P. A. McClarty, Reports on Progress in Physics **77**, 056501 (2014).
[22] J. Knolle and R. Moessner, Annual Review of Condensed Matter Physics **10**, 451 (2019).
[23] J. S. Gardner, S. R. Dunsiger, B. D. Gaulin, M. J. P. Gingras, J. E. Greedan, R. F. Kiefl, M. D. Lumsden, W. A. MacFarlane, N. P. Raju, J. E. Sonier, I. Swainson, and Z. Tun, Physical Review Letters **82**, 1012 (1999).
[24] M. Kanada, Y. Yasui, M. Ito, H. Harashina, M. Sato, H. Okumura, and K. Kakurai, Journal of the Physical Society of Japan **68**, 3802 (1999).
[25] H. R. Molavian, P. A. McClarty, and M. J. P. Gingras, "Towards an effective spin hamiltonian of the pyrochlore spin liquid $tb_2ti_2o_7$," (2009), arXiv:0912.2957 [cond-mat.stat-mech].
[26] K. Kimura, S. Nakatsuji, J.-J. Wen, C. Broholm, M. B. Stone, E. Nishibori, and H. Sawa, Nature Communications **4** (2013).
[27] Y. Tokiwa, T. Yamashita, D. Terazawa, K. Kimura, Y. Kasahara, T. Onishi, Y. Kato, M. Halim, P. Gegenwart, T. Shibauchi, S. Nakatsuji, E.-G. Moon, and Y. Matsuda, Journal of the Physical Society of Japan **87**, 064702 (2018).
[28] J.-J. Wen, S. M. Koohpayeh, K. A. Ross, B. A. Trump, T. M. McQueen, K. Kimura, S. Nakatsuji, Y. Qiu, D. M. Pajerowski, J. R. D. Copley, and C. L. Broholm, Physical Review Letters **118**, 107206 (2017).
[29] L. Savary, K. A. Ross, B. D. Gaulin, J. P. C. Ruff, and L. Balents, Physical Review Letters **109**, 167201 (2012).

[30] J. Robert, E. Lhotel, G. Remenyi, S. Sahling, I. Mirebeau, C. Decorse, B. Canals, and S. Petit, Physical Review B **92**, 064425 (2015).
[31] I. D. Ryabov, Journal of Magnetic Resonance **140**, 141 (1999).
[32] S. H. Curnoe, Physical Review B **88**, 014429 (2013).
[33] K. A. Ross, L. Savary, B. D. Gaulin, and L. Balents, Physical Review X **1**, 021002 (2011).